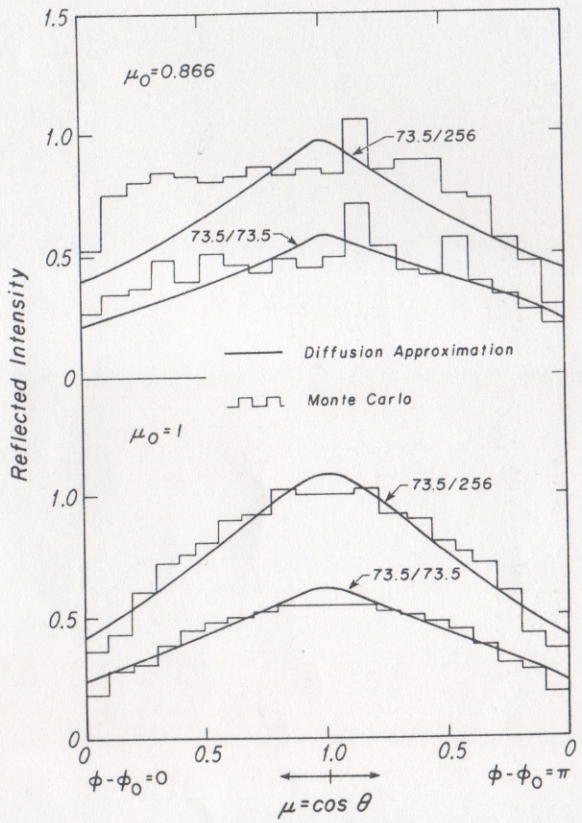

FIG. 5.31 Reflected intensity averaged over ϕ_0 as a function of the emergent angle. The histogram curves are results computed from the Monte Carlo method (McKee and Cox, 1976), and the smooth solid curves are from the diffusion approximation presented in the text.

Welch (1986) have analyzed Landsat Multispectral Scanner digital data for the mapping of cumulus cloud properties. Figure 5.32 shows the cloud size distribution for the western Atlantic cumulus scene presented in Fig. 5.28. The cloud size distribution is shown as the number of clouds per 1 km^2 surface area per 1 km cloud diameter range. Cloud size distribution is similar to the cloud droplet size distribution in which the normalization of droplets per unit volume is replaced by the normalization of clouds per unit surface area. The cloud amount varies according to the threshold method employed in the analysis. The cumulus cloud size appears to follow closely a power-law relationship with respect to the cloud diameter, except for very small sizes.

Using the Monte Carlo method, Aida (1977) has investigated the effects of cloud dimensions and orientations on the scattering pattern, assuming rectangularly shaped finite clouds. In particular, Aida showed that the clouds surrounding

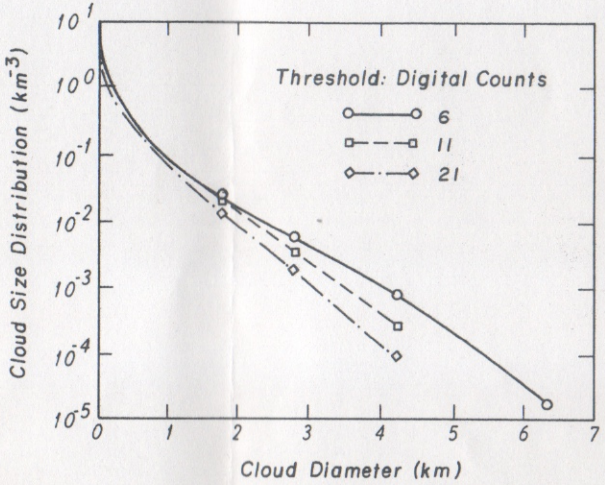

FIG. 5.32 Cloud size distribution for the western Atlantic cloud field. Values are given as the number of clouds per 1 km^2 surface area per 1 km cloud size class interval. Three curves denote results derived from different threshold methods (after Wielicki and Welch, 1986).

a cloud that is illuminated by the sun have significant interactions, if the cloud distances are within about five times their sizes. Weinman and Harshvardhan (1982) have also illustrated the importance of an array of horizontally finite clouds on solar reflection. The effects of an array of cuboidal clouds on the sensitivity of clouds on climate have been investigated by Harshvardhan (1982). While these illustrations are interesting, a realistic and quantitative assessment of the cloud horizontal nonhomogeneity with respect to the question of cloud albedo has yet to be developed.

5.5 Radiative transfer in an anisotropic medium

Cirrus clouds are composed of hexagonal ice crystals, whose single-scattering properties differ significantly from those computed for spherical particles. Figure 5.33(a) displays a number of optical phenomena in the presence of cirrus clouds at the South Pole (Greenler, 1980). Shown are 22° and 46° halos, sundogs, the parhelic circle, the circumzenithal arc of the 46° halo, and the upper tangent arc of the 22° halo. These optical features are produced by hexagonal ice plates and columns having a preferred orientation, that is, with their major axes oriented horizontally. Ice crystal habits in cirrus clouds have been presented in Fig. 4.11. With the exception of the 22° and 46° halos, which can be generated by randomly oriented ice crystals in three dimensional space, the majority of ice crystal optics are associated with the horizontal orientation of hexagonal columns and plates.

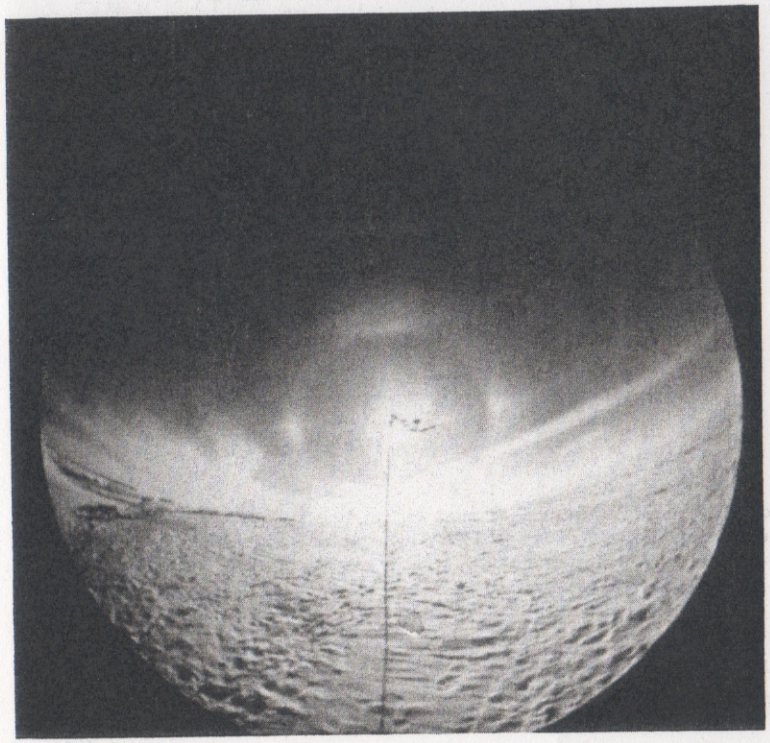

FIG. 5.33(a) Halos and arcs produced by horizontally oriented ice crystals (after Greenler, 1980). Shown are 22° and 46° halos, sundogs, the parhelic circle, the circumzenithal arc of the 46° halo and the upper tangent arc of the 22° halo.

5.5.1 *Theory*

In the case of horizontally oriented ice crystals, the single-scattering parameters depend on the direction of the incident light beam. Thus, the conventional formulation for the multiple-scattering problem is no longer applicable. Liou (1980) has formulated the basic equation for the transfer of solar radiation in an optically anisotropic medium, in which the single-scattering properties vary with the incident angle of the light beam. Stephens (1980) and Asano (1983) have discussed the transfer of radiation through optically anisotropic ice clouds. The latter author used a hypothetical cloud model in which the scattering phase function was expressed in terms of the incident angle. Takano and Liou (1989b) have included realistic scattering parameters for horizontally oriented ice crystals in their discussion and analysis. The Stokes vector was also properly accounted for in the formulation.

Let the directions of incoming and outgoing light beams be denoted by (μ', ϕ') and (μ, ϕ), respectively, where μ is the cosine of the zenith angle and ϕ is the corresponding azimuthal angle. The scattering phase matrix $\mathbf{P}$ is a function of

(μ, ϕ, μ', ϕ') and cannot be defined by the scattering angle Θ alone, as in conventional radiative transfer. Moreover, the extinction (σ_e) and scattering (σ_s) cross sections vary with the direction of the incoming light beam (μ', ϕ').

Consider an anisotropic medium consisting of ice crystals randomly oriented in a horizontal plane. Because of the symmetry with respect to the azimuthal angle for the incoming light beam, the phase matrix and the extinction and scattering cross sections may be expressed by $\mathbf{P}(\mu, \phi, \mu', \phi') = \mathbf{P}(\Theta, \Phi, \mu')$, $\sigma_e(\mu')$, and $\sigma_s(\mu')$, respectively, where Φ is the azimuthal angle associated with the scattering angle Θ. In this case, we may define the differential normal optical depth in the form

$$\frac{d\tilde{\tau}}{dz} = -\tilde{\sigma}_e N, \tag{5.5.1}$$

where the normal extinction cross section, $\tilde{\sigma}_e = \sigma_e(\mu' = 1)$, N is the number density of the particles, and z is the distance. Let the Stokes vector intensity $\mathbf{I} = (I, Q, U, V)$. The general equation governing the transfer of diffuse solar intensity may be written in the form

$$\mu \frac{d\mathbf{I}(\tilde{\tau}; \mu, \phi)}{d\tilde{\tau}} = \mathbf{I}(\tilde{\tau}; \mu, \phi)k(\mu) - \mathbf{J}(\tilde{\tau}; \mu, \phi), \tag{5.5.2}$$

where

$$k(\mu) = \sigma_e(\mu)/\tilde{\sigma}_e, \tag{5.5.3}$$

and the source function

$$\mathbf{J}(\tilde{\tau}; \mu, \phi) = \frac{1}{4\pi} \int_0^{2\pi} \int_{-1}^{1} \tilde{\omega}(\mu')\mathbf{P}(\mu, \phi; \mu', \phi')\mathbf{I}(\tilde{\tau}; \mu', \phi')\, d\mu'\, d\phi' + \frac{1}{4\pi}\tilde{\omega}(-\mu_0)\mathbf{P}(\mu, \phi; -\mu_0, \phi_0)\mathbf{F}_\odot \exp[-k(-\mu_0)\tilde{\tau}/\mu_0]. \tag{5.5.4}$$

The first and second terms on the right-hand side represent contributions from, respectively, the multiple and single scattering of the direct solar intensity. The equivalent single-scattering albedo is defined as

$$\tilde{\omega}(\mu) = \sigma_s(\mu)/\tilde{\sigma}_e. \tag{5.5.5}$$

The general phase matrix, with respect to the local meridian plane, is given by (Liou, 1980)

$$\mathbf{P}(\mu, \mu'; \phi - \phi') = \mathbf{L}(\pi - i_2)\mathbf{P}(\Theta, \Phi, \mu')\mathbf{L}(-i_1), \tag{5.5.6}$$

where i_1 and i_2 denote the angles between the meridian planes for the incoming and outgoing light beams, respectively, and the plane of scattering, as illustrated

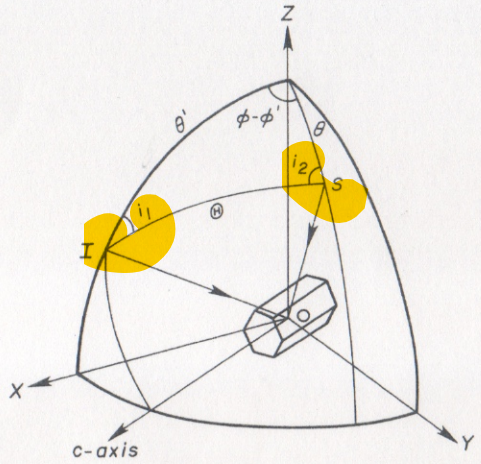

FIG. 5.33(b) Scattering geometry involving horizontally oriented ice crystals. The terms IO and SO denote the incident (θ', ϕ') and scattered (θ, ϕ) directions, respectively. i_1 and i_2 are angles between the meridian planes for the incoming and scattered light beams, respectively. The scattering angle is denoted by Θ.

in Fig. 5.33(b). The transformation matrix for the Stokes vector is given by [see also Eq. (5.1.38)]

$$\mathbf{L}(\chi) = \begin{bmatrix} 1 & 0 & 0 & 0 \\ 0 & \cos 2\chi & \sin 2\chi & 0 \\ 0 & -\sin 2\chi & \cos 2\chi & 0 \\ 0 & 0 & 0 & 1 \end{bmatrix}, \tag{5.5.7}$$

where $\chi = -i_1$ or $\pi - i_2$. From spherical geometry, these angles are given by

$$\cos i_1 = \frac{-\mu + \mu' \cos\Theta}{\pm(1 - \cos^2\Theta)^{1/2}(1-\mu^2)^{1/2}}, \tag{5.5.8}$$

$$\cos i_2 = \frac{-\mu' + \mu \cos\Theta}{\pm(1 - \cos^2\Theta)^{1/2}(1-\mu^2)^{1/2}}. \tag{5.5.9}$$

If $\mathbf{P}(\Theta, \Phi, \mu)$, $\sigma_e(\mu)$, and $\sigma_s(\mu)$ are known, then, in principle, Eq. (5.5.2) may be solved numerically.

We shall approach the multiple-scattering problem by means of the adding-method for radiative transfer described in Section 3.2.2. To proceed with the adding principle for radiative transfer in an anisotropic medium, we utilize the reflection and transmission matrices defined in Section 3.2.2 and consider an infinitesimal layer with a very small optical depth $\Delta\tilde{\tau}$, say 10^{-8}. Since the optical depth is so small, only single scattering takes place within the layer. From Eqs. (5.5.2) and

(5.5.4), the analytic solutions for the reflected and transmitted intensities undergoing single scattering may be derived. Subject to the condition that $\Delta\tilde{\tau} \to 0$, we find

$$\mathbf{T}(\mu, \mu_0; \phi - \phi_0) \cong \frac{\Delta\tilde{\tau}}{4\mu\mu_0}\tilde{\omega}(\mu_0)\mathbf{P}(\mu, \mu_0; \phi - \phi_0), \tag{5.5.10}$$

$$\mathbf{R}(\mu, \mu_o; \phi - \phi_0) \cong \frac{\Delta\tilde{\tau}}{4\mu\mu_0}\tilde{\omega}(\mu_0)\mathbf{P}(-\mu, \mu_0; \phi - \phi_0), \tag{5.5.11}$$

$$\mathbf{T}^*(\mu, \mu_0; \phi - \phi_0) \cong \frac{\Delta\tilde{\tau}}{4\mu\mu_0}\tilde{\omega}(\mu_0)\mathbf{P}(-\mu, -\mu_0; \phi - \phi_0), \tag{5.5.12}$$

$$\mathbf{R}^*(\mu, \mu_0; \phi - \phi_0) \cong \frac{\Delta\tilde{\tau}}{4\mu\mu_0}\tilde{\omega}(\mu_0)\mathbf{P}(\mu, -\mu_0; \phi - \phi_0). \tag{5.5.13}$$

where the phase matrix $\mathbf{P}$ has been defined in Eq. (5.5.6).

With modifications to account for the dependence of the optical properties on the incoming direction, the procedure for computing the reflection and transmission matrices for the composite layer may be described by the following equations:

$$\mathbf{Q}_1 = \mathbf{R}_a^* \mathbf{R}_b, \tag{5.5.14}$$

$$\mathbf{Q}_n = \mathbf{Q}_1 \mathbf{Q}_{n-1}, \tag{5.5.15}$$

$$\mathbf{S} = \sum_{n-1}^{M} \mathbf{Q}_n, \tag{5.5.16}$$

$$\mathbf{D} = \mathbf{T}_a + \mathbf{S}\exp[-k(\mu_0)\tilde{\tau}_a/\mu_0] + \mathbf{S}\mathbf{T}_a, \tag{5.5.17}$$

$$\mathbf{U} = \mathbf{R}_b \exp[-k(\mu_0)\tilde{\tau}_a/\mu_0] + \mathbf{R}_b\mathbf{D}, \tag{5.5.18}$$

$$\mathbf{R}_{a,b} = \mathbf{R}_a + \exp[-k(\mu)\tilde{\tau}_a/\mu]\mathbf{U} + \mathbf{T}_a^*\mathbf{U}, \tag{5.5.19}$$

$$\mathbf{T}_{a,b} = \exp[-k(\mu)\tilde{\tau}_b/\mu]\mathbf{D} + \mathbf{T}_b \exp[-k(\mu_0)\tilde{\tau}_a/\mu_0] + \mathbf{T}_b\mathbf{D}. \tag{5.5.20}$$

The exponential terms in the adding equations denote the direct transmission through layer a or b without scattering, where the anisotropic factor $k(\mu)$ is given in Eq. (5.5.3). The total transmission for the combined layer is the sum of the diffuse transmission $\mathbf{T}_{a,b}$ and the direct transmission, $\exp[-k(\mu_0)(\tilde{\tau}_a + \tilde{\tau}_b)/\mu_0]$, in the direction of the sun.

In order to compute the reflection and transmission matrices for the initial layer with a very small optical depth, via Eqs. (5.5.10)–(5.5.13), we need the phase matrix and single-scattering albedo, and the directions of the incoming and outgoing beams. The phase matrix elements must be expanded in terms of the incoming and outgoing directions denoted by μ, μ' and $\phi - \phi'$. For spherical particles, the phase matrix consists of four nonzero independent elements. These elements can be decoupled analytically in terms of functions associated with μ, μ' and $\phi - \phi'$ (Dave, 1970; Kattawar et al., 1973). However, for nonspherical particles,the decomposition of the phase matrix elements has yet to be worked out. For randomly oriented nonspherical particles that have a plane of symmetry, the phase matrix

contains six independent elements. In this case, there are seven symmetrical relationships for these elements based on the reciprocity principle (Hovenier, 1969). From these relationships, the phase matrix elements can be expanded in terms of either cosine or sine Fourier components (Hansen, 1971). For randomly oriented ice plates or columns in a horizontal plane, there are 16 elements in the phase matrix. It can be proved that these elements obey a number of symmetrical relationships, based on which they can be expanded in terms of either cosine or sine Fourier components.

In view of the above discussion, the general phase matrix elements may be numerically expanded in the forms

$$\tilde{\omega}(\mu')P_{ij}(\mu,\mu';\phi-\phi') = P_{ij}^0(\mu,\mu')+2\sum_{m=1}^{N} P_{ij}^m(\mu,\mu')\times\begin{cases}\cos m(\phi-\phi'), & c\\ \sin m(\phi-\phi'), & s,\end{cases} \tag{5.5.21}$$

where

$$c, \quad ij = 11, 12, 21, 22, 33, 34, 43, 44$$

$$s, \quad ij = 13, 14, 23, 24, 31, 32, 41, 42$$

and $P_{ij}^m (m = 0, 1, ..., N)$ denotes the Fourier expansion coefficients. With this expansion, each term in the Fourier series may be treated independently in numerical computations. For spherical particles or randomly oriented nonspherical particle, Eq. (5.5.21) can be used except that $\tilde{\omega}(\mu') = 1$.

With respect to the normalization of the phase function P_{11}, the following procedures may be used. The phase function is normalized such that

$$\frac{1}{4\pi}\int_0^{2\pi}\int_{-1}^{1} P_{11}(\mu,\mu',\phi-\phi')\,d\mu\,d(\phi-\phi') = 1, \tag{5.5.22a}$$

where $d\mu\,d(\phi-\phi')$ denotes the differential solid angle. Using Eq. (5.5.21), we find

$$\frac{1}{2}\int_{-1}^{1} P_{11}^0(\mu,\mu')\,d\mu = \tilde{\omega}(\mu'), \tag{5.5.22b}$$

where $\tilde{\omega}(\mu')$ is defined in Eq. (5.5.5). In the case of randomly oriented nonspherical particles (or spherical particles), the single-scattering albedo $\tilde{\omega}$ is independent of μ' and is a constant. If there is no absorption, $\tilde{\omega} = 1$. In this case, Eq. (5.5.22b) can be derived from the expansion of the phase function in terms of the Legendre polynomial using the addition theorem for spherical harmonics (Liou, 1980). However, for randomly oriented ice crystals in a horizontal plane, $\tilde{\omega}$ is a function of the incident angle. Normalization of the phase function must be performed for each μ'.

The phase function P_{11} for ice crystals has a common sharp diffraction peak. In order to account for this peak in numerical integrations properly, thousands of

Fourier components are needed in the phase function expansion. To optimize the computational effort, the procedure proposed by Potter (1970) may be followed. In this procedure, the forward peak is truncated by extrapolating the phase function linearly from the scattering angles 10° to 0° in the logarithmic scale. Let the truncated phase function be P_{11}^t; then the truncated fraction of scattered intensity is given by

$$f = \int_{4\pi} (P_{11} - P_{11}^t)\,d\Omega/4\pi. \tag{5.5.23}$$

To use the truncated phase function in multiple-scattering computations while, at the same time, achieving the "equivalent" result, as in the case when the sharp diffraction peak was included in the computations, an adjustment must be made for the optical depth and single-scattering albedo in a manner described in Section 3.6.

5.5.2 *Effects of horizontal orientation of ice crystals on cloud radiative properties*

In order to compute the reflected and transmitted intensity of sunlight from oriented ice crystals, the phase function is required. The phase functions for horizontally oriented plates and columns have been computed by Takano and Liou (1989a) using the geometric ray-tracing technique. The phase function is a function of the incoming direction (μ, ϕ) and the outgoing direction (μ', ϕ'). The computations of the phase function for oriented two-dimensional (2D) plates (randomly oriented with their c axis vertical), Parry columns (the c axis and a pair of prisms facing horizontal), and 2D columns (the c axis horizontal with random rotational orientation about this c axis) lead to the interpretation of numerous halos and arcs observed in the atmosphere. Figure 5.34 illustrates the reflected and transmitted intensity patterns for 2D plates when the solar zenith angle, θ_0, is 75°. The optical depth presented in this graph is a mean value averaged over the zenith angle θ. In the case of 2D plates, scattered sunlight is confined to four latitude belts, due to specific geometry. Based on the ray-tracing geometry for plates, the emergent zenith angle may be computed from the incoming solar zenith angle θ_0, in the forms

$$\theta^* = \begin{cases}\pi/2 - \sin^{-1}(m_r^2 - \sin^2\theta_0)^{1/2}, & \text{for } \theta_0 > \sin^{-1}(m_r^2-1)^{1/2} \simeq 58^\circ\\ \sin^{-1}(m_r^2 - \cos^2\theta_0)^{1/2}, & \text{for } \theta_0 < \cos^{-1}(m_r^2-1)^{1/2} \simeq 32^\circ.\end{cases} \tag{5.5.24}$$

For $\theta_0 = 75°$, these latitude belts correspond to zenith angles of ±75° and ±27°,with negative values representing mirror images. If the incident angle is 27°, the four latitude belts are ±27° and ±75°. Due to the symmetrical property of 2D plates with respect to incoming light beams, all multiply scattered light is also confined to the four latitude belts. The reflected and transmitted intensities for optical depths 1/4, 1, 4, and 16 are displayed as a function of the azimuthal

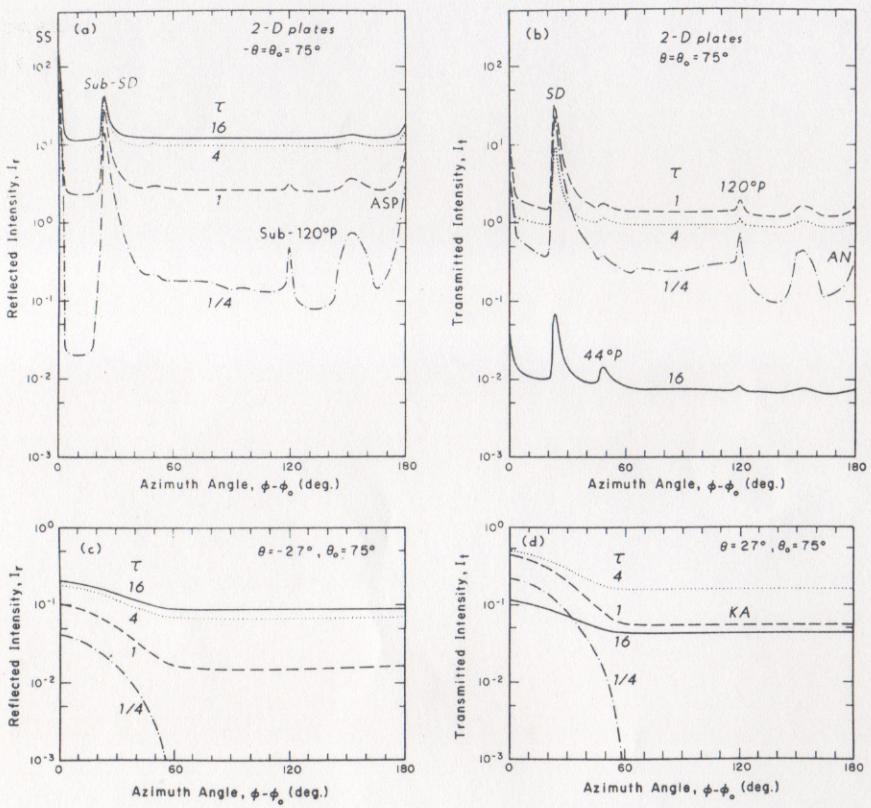

FIG. 5.34 Intensity of sunlight reflected and transmitted by 2D plates ($L/2r = 0.1$) as a function of the azimuth angle, $\phi - \phi_0$, for (a) $\theta = -\theta_0 = -75°$, (b) $\theta = \theta_0 = 75°$, (c) $(\theta, \theta_0) = (-27°, 75°)$ and (d) $(\theta, \theta_0) = (27°, 75°)$. The optical depth τ in 2D cases is a value averaged over all directions ($0 \leq \mu \leq 1$) (after Takano and Liou, 1989b).

angle, $\phi - \phi_0$. The reflected intensity increases with increasing optical depth. For the 75° emergent zenith angle, the subsun, subsundog, 120° subparhelion, and antisolar peak optical features are shown distinctly for an optical depth of 1/4, at which single scattering dominates. For an optical depth of 16, only the subsun and subparhelion are observed. For the transmitted intensity, the sundog is visible even for large cloud optical depths. In addition to these optical phenomena, the anthelion (AN) located at the 180° azimuthal angle is seen for the small optical depth of 1/4, due to double scattering, viz., the coupling of the subsun and antisolar peak. For an optical depth of 16, the 44° parhelion produced by double scattering (denoted as 44°P) is also observed. At the 27° zenith angle, the Kern's arc (KA) appears for $\tau \geq 1$ due to the effects of multiple scattering.

Figures 5.35 and 5.36 display the reflected and transmitted intensity patterns as a function of the zenith angle on the plane $\phi - \phi_0 = 0°$ for Parry and 2D columns,

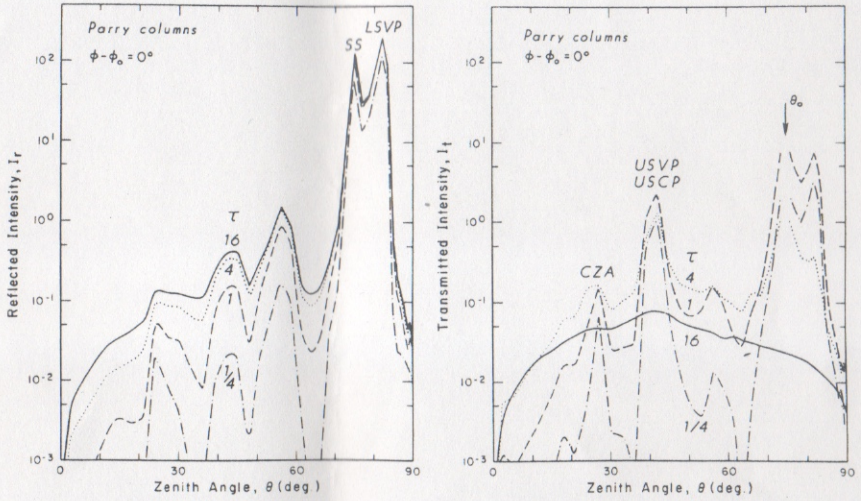

FIG. 5.35 Intensity of sunlight reflected and transmitted by Parry columns ($L/2r = 2.5$) in the solar principal plane ($\phi - \phi_0 = 0°$) at $\lambda = 0.5$ μm. The solar zenith angle is 75° (after Takano and Liou, 1989b).

respectively. The solar zenith angle used for the computation is 75°. These patterns for an optical depth of 1/4 are basically similar to those from single-scattering computations, except for the subpeak at $\theta = 82°$ in the transmitted intensity in Fig. 5.35. This peak is caused by the lower sunvex Parry arc of the subsun. For Parry columns, several optical features are observed for optical depths less than 4. These include the subsun (SS) and lower sunvex Parry arc (LSVP) in

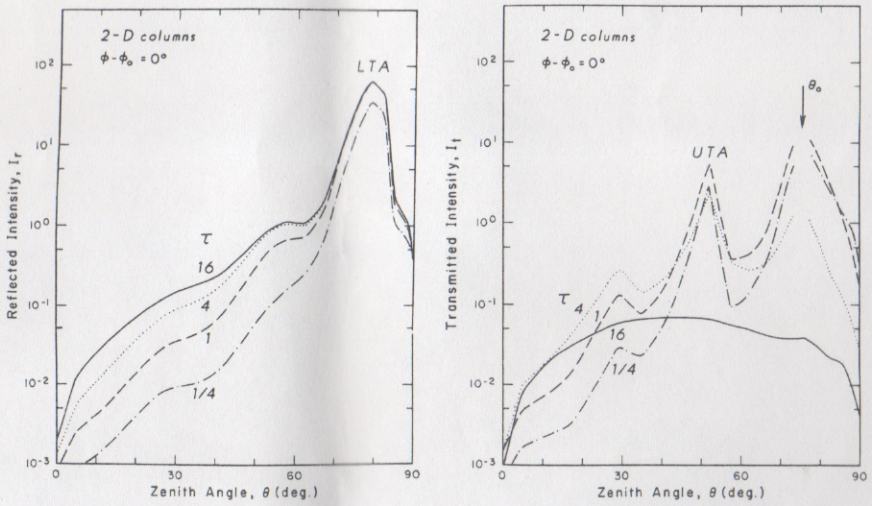

FIG. 5.36 As in Fig. 5.35, except for 2D columns ($L/2r = 2.5$) (after Takano and Liou, 1989b).

the reflected intensity (these are also visible for an optical depth of 16), and the circumzenith arc (CZA) and upper suncave (USCP) and sunvex (USVP) Parry arcs in the transmitted intensity. For 2D columns, the lower tangent arc (LTA) is noticeable in the reflected intensity for all optical depths. When the optical depth is large, the transmitted intensities have the lowest values in the zenith and nadir directions, as shown in Figs. 5.35 and 5.36. Except for these features, the reflected and transmitted intensities of 2D columns are similar to those of randomly oriented columns. Also, it is noted that the reflected and transmitted intensity distributions of Parry columns are similar to those of 2D columns for large optical depths ($\tau = 16$) because sufficient multiple scattering is present. Optical phenomena produced by 2D plates, Parry columns, and 2D columns and their causes are listed in Table 5.5. The causes of the frequently observed halos and arcs produced by horizontally oriented columns and plates are illustrated in Fig. 5.37, in which the rays that are required to generate these optics are displayed.

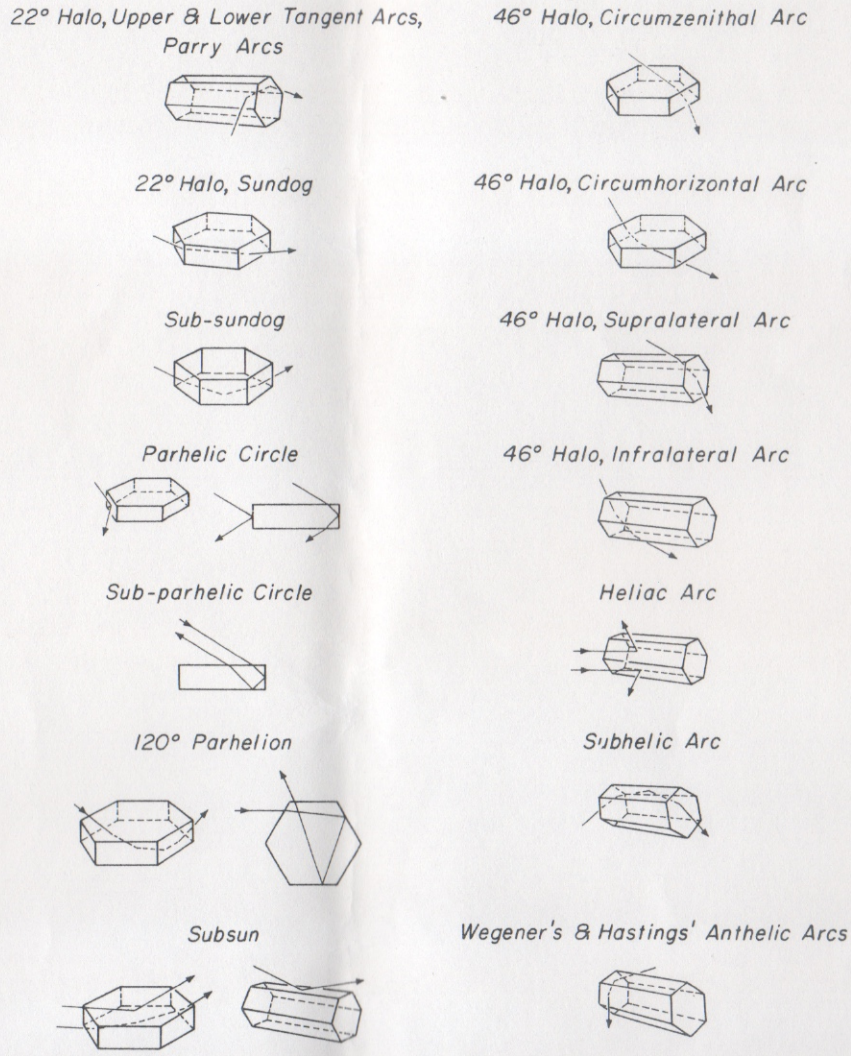

FIG. 5.37 The causes of frequently observed halos and arcs produced by horizontally oriented columns and plates (a summary of the displays illustrated in Greenler, 1980).

Table 5.5 Optical phenomena caused by 2D plates, Parry columns, and 2D columns[a]

Abbreviation	Definition
	2D Plates
ASP	antisolar peak
CHA	circumhorizontal arc
CZA	circumzenithal arc
ER	external reflection
KA	Kern's arc
120° P	120° parhelion
120° Sub-P	120° subparhelion
PC	parhelic circle
SD	sundog (22° parhelion)
SS	subsun
Sub-CHA	subcircumhorizontal arc
Sub-CZA	subcircumzenithal arc
Sub-SD	sub-sundog (22° subparhelion)
	Parry Columns
ASA	antisolar arc
ASP	antisolar peak
CZA	circumzenithal arc
HA	heliac arc
HAA	Hastings' anthelic arc
LSCP	lower suncave Parry arc
LSVP	lower sunvex Parry arc
PC	parhelic circle
SHA	subhelic arc
SID	solar incident direction
SS	subsun
Sub-CZA	subcircumzenithal arc
Sub-PC	subparhelic circle
USCP	upper suncave Parry arc
SUVP	upper sunvex Parry arc
	2D Columns
ASA	antisolar arc
ASP	antisolar peak
DA	diffuse arc
ILA	infralateral arc
LTA	lower tangent arc
PC	parhelic circle
SHA	subhelic arc
SID	solar incident direction
SLA	supralateral arc
TAA	Tricker's anthelic arc
UTA	upper tangent arc
WAA	Wegener's anthelic arc

[a] After Takano and Liou (1989a).

REFERENCES

Aida, M., 1977: Scattering of solar radiation as a function of cloud dimensions and orientation. *J. Quant. Spectrosc. Radiat. Transfer*, **17**, 303–310.

Asano, S., 1983: Transfer of solar radiation in optically anisotropic ice clouds. *J. Meteor. Soc. Japan*, **61**, 402–413.

Asano, S., and G. Yamamoto, 1975: Light scattering by a spheroidal particle. *Appl. Opt.*, **14**, 29–49.

Asano, S., and M. Sato, 1980: Light scattering by randomly oriented spheroidal particles. *Appl. Opt.*, **19**, 962–974.

Barber, P., and C. Yeh, 1975: Scattering of electromagnetic waves by arbitrarily shaped dielectric bodies. *Appl. Opt.*, **14**, 2864–2872.

Berg, P. W., and J. L. McGregor, 1966: *Elementary Partial Differential Equations*. Holden-Day, Inc., San Francisco, 421 pp.

Bertie, J. E., H. J. Labbé, and E. Whalley, 1969: Absorptivity of ice I in the range of 4000–30 cm^{-1}. *J. Chem. Phys.*, **50**, 4501–4520.

Blau, H. H., R. P. Espinola, and E. C. Reifenstein, 1966: Near infrared scattering by sunlit terrestrial clouds. *Appl. Opt.*, **5**, 555–564.

Bohren, C. F., and D. R. Huffman, 1983: *Absorption and Scattering of Light by Small Particles*. Wiley, New York, 530 pp.

Born, M., and E. Wolf, 1975: *Principles of Optics*. Pergamon Press, Oxford, 808 pp.

Busygin, V. P., N. A. Yevstratov, and Ye. M. Feygel'son, 1973: Optical properties of cumulus clouds, and radiant fluxes for cumulus cloud cover. *Izv. Acad. Sci. USSR Atmos. Ocean. Phys.*, **9**, 1142–1151.

Cai, Q., and K. N. Liou, 1982: Polarized light scattering by hexagonal ice crystals: Theory. *Appl. Opt.*, **21**, 3569–3580.

Case, K., and P. F. Zweifel, 1967: *Linear Transport Theory*. Addison-Wesley, Reading, Mass., 342 pp.

Coffeen, D. L. 1979: Polarization and scattering characteristics in the atmosphere of Earth, Venus, and Jupiter. *J. Opt. Soc. Amer.*, **69**, 1051–1064.

Coleman, R. F., and K. N. Liou, 1981: Light scattering by hexagonal ice crystals. *J. Atmos. Sci.*, **38**, 1260–1271.

Crosbie, A. L., and T. L. Linsenbardt, 1978: Two-dimensional isotropic scattering in a semi-infinite medium. *J. Quant. Spectrosc. Radiat. Transfer*, **19**, 257–284.

Dave, J. V., 1970: Coefficients of the Legendre and Fourier series for the scattering functions of spherical particles. *Appl. Opt.*, **9**, 1888–1896.

Davies, R., 1978: The effect of finite geometry on the three-dimensional transfer of solar irradiance in clouds. *J. Atmos. Sci.*, **35**, 1712–1725.

Deirmendjian, D., 1969: *Electromagnetic Scattering on Spherical Polydispersions*. Elsevier, New York, 291 pp.

Dugin, V. P., and S. O. Mirumyants, 1976: The light scattering matrices of artificial crystalline clouds. *Izv. Acad. Sci. USSR Atmos. Ocean. Phys.*, **12**, 988–991.

Foot, J. S., 1988a: Some observations of the optical properties of clouds. I. Stratocumulus. *Quart. J. Roy. Meteor. Soc.*, **114**, 129–144.

Foot, J. S., 1988b: Some observations of the optical properties of clouds. II. Cirrus. *Quart. J. Roy. Meteor. Soc.*, **114**, 145–164.

Giovanelli, R. G., 1959: Radiative transfer in a non-uniform media. *Aust. J. Phys.*, **12**, 164–170.

Greenberg, J. M., A. C. Lind, R. T. Wang, and L. F. Libelo, 1967: Scattering by nonspherical system. In *Electromagnetic Scattering*, R. L. Rowell and F. S. Stein, Eds., Gordon and Breach, New York, pp. 3-54.

Greenler, R., 1980: *Rainbows, Halos, and Glories*. Cambridge University Press, Cambridge, 195 pp.

Griffith, K. T., S. K. Cox, and R. G. Knollenberg, 1980: Infrared radiative properties of tropical cirrus clouds inferred from aircraft measurements. *J. Atmos. Sci.*, **37**, 1077–1087.

Hale, G. M., and M. R. Querry, 1973: Optical constants of water in the 200-μm to 200-nm wavelength region. *Appl. Opt.*, **12**, 555–563.

Hansen, J. E., 1971: Multiple scattering of polarized light in panetary atmospheres. Parts I and II. *J. Atmos. Sci.*, **28**, 120–125, 1400–1426.

Hansen, J. E., and J. B. Pollack, 1970: Near-infrared light scattering by terrestrial clouds. *J. Atmos. Sci.*, **27**, 265–281.

Harshvardhan, 1982: The effect of brokeness on cloud-climate sensitivity. *J. Atmos. Sci.*, **39**, 1853–1861.

Herman, G. F., and J. A. Curry, 1984: Observational and theoretical studies of solar radiation in arctic stratus clouds. *J. Climate Appl. Meteor.*, **23**, 5–24.

Hobbs, P. V., 1974: *Ice Physics*, Oxford University Press, London, 835 pp.

Hovenier, J. W., 1969: Symmetry relationships for scattering of polarized light in a slab of randomly oriented particles. *J. Atmos. Sci.*, **26**, 488–499.

Irvine, W. M., and J. B. Pollack, 1968: Infrared optical properties of water and ice spheres. *Icarus*, **8**, 324–360.

Iskander, M.F., A. Lakhtakia, and C. Durney, 1983: A new procedure for improving the solution stability and extending the frequency range of the EBCM. *IEEE Trans. Antennas and Propagat.*, **AP-31**, 317–324.

Jacobowitz, H., 1971: A method for computing transfer of solar radiation through clouds of hexagonal ice crystals. *J. Quant. Spectrosc. Radiat. Transfer*, **11**, 691–695.

Kattawar, G. W., S. J. Hitzfelder, and J. Binstock, 1973: An explicit form of the Mie phase matrix for multiple scattering calculations in the I, Q, U, and V representation. *J. Atmos. Sci.*, **30**, 289–295.

Kerker, M., 1969: *The Scattering of Light and Other Electromagnetic Radiation*. Academic Press, New York, 666 pp.

King, M. D., L. F. Radke, and P. V. Hobbs, 1990: Determination of the spectral absorption of solar radiation by marine stratocumulus clouds from airborne measurements within clouds. *J. Atmos. Sci.*, **47**, 894–907.

Kinne, S., and K. N. Liou, 1989: The effects of the nonsphericity and size distribution of ice crystals on the radiative properties of cirrus clouds. *Atmos. Res.*, **24**, 273–284.

Liou, K. N., 1972: Light scattering by ice clouds in the visible and infrared: A theoretical study. *J. Atmos. Sci.*, **29**, 524–536.

Liou, K. N., 1976: On the absorption, reflection and transmission of solar radiation in cloudy atmospheres. *J. Atmos. Sci.*, **33**, 798–805.

Liou, K. N., 1980: *An Introduction to Atmospheric Radiation*. Academic Press, New York, 392 pp.

Liou, K. N., 1986: Influence of cirrus clouds on weather and climate processes: A global perspective. *Mon. Wea. Rev.*, **114**, 1167–1199.

Liou, K. N., and S. C. Ou, 1979: Infrared radiative transfer in finite cloud layers. *J. Atmos. Sci.*, **36**, 1985–1996.

Liou, K. N., and G. D. Wittman, 1979: Parameterization of the radiative properties of clouds. *J. Atmos. Sci.*, **36**, 1261–1273.

Lord Rayleigh, 1918: The dispersal of light by a dielectric cylinder. *Phil. Mag.*, **36**, 365–376.

Mckee, T., and S. K. Cox, 1976: Simulated radiance patterns for finite cubic clouds. *J. Atmos. Sci.*, **33**, 2014–2020.

Mie, G., 1908: Beiträge zur Optik trüber Medien, speziell kolloidaler Metallösungen. *Ann. Physik*, **25**, 377–445.

Muinonen, K., K. Lumme, J. Peltoniemi, and W. M. Irvine, 1989: Light scattering by randomly oriented crystals. *Appl. Opt.*, **28**, 3051–3060.

Nikiforova, N. K., L. N. Pavlova, A. G. Petrushin, V. P. Snykov, and O. A. Volkovitsky, 1977: Aerodynamic and optical properties of ice crystals. *J. Aerosol Sci.*, **8**, 243–250.

Ou, S. C., and K. N. Liou, 1980: Numerical experiments on the Helmholtz equation derived from the solar radiation transfer equation in three-dimensional space. *Appl. Math. Comp.*, **7**, 155–175.

Ou, S. C., and K. N. Liou, 1982: Generalization of the spherical harmonic method to radiative transfer in multi-dimensional space. *J. Quant. Spectrosc. Radiat. Transfer*, **28**, 271–288.

Paltridge, G. W., and C. M. R. Platt, 1981: Aircraft measurements of solar and infrared radiation and the microphysics of cirrus clouds. *Quart. J. Roy. Meteor. Soc.*, **107**, 367–380.

Perrin, F., 1942: Polarization of light scattered by isotropic opalescent media. *J. Chem. Phys.*, **10**, 415–527.

Plank, V. G., 1969: The size distribution of cumulus clouds in representive Florida populations. *J. Appl. Meteor.*, **8**, 46–67.

Platt, C. M. R., 1976: Infrared absorption and liquid water content in stratocumulus clouds. *Quart. J. Roy. Meteor. Soc*, **102**, 553–561.

Pollack, J. B., D. W. Strecker, F. C. Witteborn, E. F. Erickson, and B. J. Baldwin, 1978: Properties of the clouds of Venus, as inferred from airborne observations of its near-infrared reflective spectrum. *Icarus*, **23**, 28–45.

Potter, J. F., 1970: The delta function approximation in radiative transfer theory. *J. Atmos. Sci.*, **27**, 943–951.

Reynolds, D. W., T. H. Vonder Haar, and S. K. Cox, 1975: The effect of solar radiation absorption in the tropical troposphere. *J. Appl. Meteor.*, **14**, 433–443.

Roewe, D., and K. N. Liou, 1978: Influence of cirrus clouds on the infrared cooling rate in the troposphere and lower stratosphere. *J. Appl. Meteor.*, **17**, 92–106.

Rozenberg, G., M. Malkevich, V. Malkova, and V. Syachinov, 1974: Determination of the optical characteristics of clouds from measurements of reflected solar radiation by KOSMOS 320. *Izv. Acad. Sci. USSR Atmos. Ocean. Phys.*, **10**, 14–24.

Sassen, K., and K. N. Liou, 1979: Scattering of polarized laser light by water droplet, mixed phase, and ice crystal clouds: I. Angular scattering patterns. *J. Atmos. Sci.*, **36**, 838–851.

Schaaf, J. W., and D. Williams, 1973: Optical constants of ice in the infrared. J. *Opt. Soc. Amer.*, **63**, 726–732.

Seki, M., K. Kobayashi, and J. Nakahara, 1981: Optical spectra of hexagonal ice. *J. Phys. Soc. Japan*, **50**, 2643–2648.

Slingo, A., 1989: A GCM parameterization for the shortwave radiative properties of water clouds. *J. Atmos. Sci.*, **46**, 1419–1427.

Smith, W. L., Jr., P. F. Hein, and S. K. Cox, 1990: The 27–28 October 1986 FIRE IFO cirrus case study: In situ observations of radiation and dynamic propterties of a cirrus cloud layer. *Mon. Wea. Rev.*, **118**, 2389–2401.

Spänkuch, D., and W. Döhler, 1985: Radiative properties of cirrus clouds in the middle ir derived from Fourier spectrometer measurements from space. *Z. Meteor.*, **6**, 314–324.

Stephens, G. L., 1978: Radiation profiles in extended water clouds. II. Parameterization schemes. *J. Atmos. Sci.*, **35**, 2123–2132.

Stephens, G. L., 1980: Radiative transfer on a linear lattice: Application to anisotropic ice crystal clouds. *J. Atmos. Sci.*, **37**, 2095–2104.

Stephens, G. L., 1984: The parameterization of radiation for numerical weather prediction and climate models. *Mon. Wea. Rev.*, **112**, 826–867.

Stephens, G. L., G. W. Paltridge, and C. M. R. Platt, 1978: Radiation profiles in extended water clouds. III: Observations. *J. Atmos. Sci.*, **35**, 2133–2141.

Stephens, G. L., and S. C. Tsay, 1990: On the cloud absorption anomaly. *Quart. J. Roy. Meteor. Soc.*, **116**, 671–704.

Takano, Y., and K. Jayaweera, 1985: Scattering phase matrix for hexagonal ice crystals computed from ray optics. *Appl. Opt.*, **24**, 3254–3263.

Takano, Y., and K. N. Liou, 1989a: Solar radiative transfer in cirrus clouds. Part I: Single-scattering and optical properties of hexagonal ice crystals. *J. Atmos. Sci.*, **46**, 3–19.

Takano, Y., and K. N. Liou, 1989b: Solar radiative transfer in cirrus clouds. Part II: Theory and computation of multiple scattering in an anisotropic medium. *J. Atmos. Sci.*, **46**, 20–36.

Twomey, S., 1976: Computations of the absorption of solar radiation by clouds. *J. Atmos. Sci.*, **33**, 1087–1091.

Twomey, S., and T. Cocks, 1982: Spectral reflectance of clouds in the near-infrared: Comparison of measurements and calculations. *J. Meteor. Soc. Japan*, **60**, 583–592.

Twomey, S., and K. J. Seton, 1980: Inferences of gross microphysical properties of clouds from spectral reflectance measurements. *J. Atmos. Sci.*, **37**, 1065–1069.

van de Hulst, H. C., 1957: *Light Scattering by Small Particles*. Wiley, New York, 470 pp.

Volkovitsky, O. A., L. N. Pavlova, and A. G. Petrushin, 1980: Scattering of light by ice crystals. *Izv. Acad. Sci. USSR. Atmos. Ocean. Phys.*, **16**, 90–102.

Vouk, V., 1948: Projected area of convex bodies. *Nature*, **162**, 330–331.

Wait, J. R., 1955: Scattering of a plane wave from a circular dielectric cylinder at oblique incidence. *Can. J. Phys.*, **33**, 189–195.

Warren, S. G., 1984: Optical constants of ice from ultraviolet to the microwave. *Appl. Opt.*, **23**, 1206–1225.

Weinman, J. A., and Harshvardhan, 1982: Solar reflection from a regular array of horizontally finite clouds. *Appl. Opt.*, **21**, 2940–2944.

Welch, R. M., S. K. Cox, and J. M. Davis, 1980: *Solar Radiation and Clouds. Meteor. Monogr.*, No. 39, Amer. Meteor. Soc., Boston, 96 pp.

Wendling, P., R. Wendling, and H. K. Weickmann, 1979: Scattering of solar radiation by hexagonal ice crystals. *Appl. Opt.*, **18**, 2663–2671.

Wielicki, B. A., and R. M. Welch, 1986: Cumulus cloud properties derived using Landsat satellite data. *J. Climate Appl. Meteor.*, **25**, 261–276.

Wiscombe, W. J., 1980: Improved Mie scattering algorithms. *Appl. Opt.*, **19**, 1505–1509.

Wiscombe, W. J., R. M. Welch, and W. D. Hall, 1984: The effects of very large drops on cloud adsorption. Part I: Parcel models. *J. Atmos. Sci.*, **41**, 1336–1355.

Zander, R., 1966: Spectral scattering properties of ice clouds and hoarfrost. *J. Geophys. Res.*, **71**, 375–378.